Report

Cell Reports

Cross-Reactive Donor-Specific CD8$^+$ Tregs Efficiently Prevent Transplant Rejection

Graphical Abstract

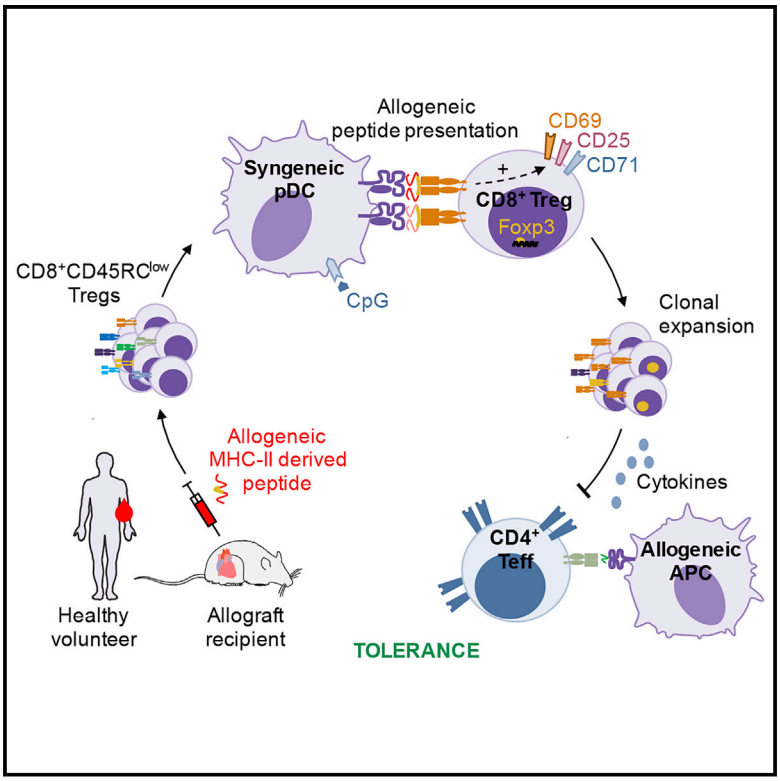

Authors

Elodie Picarda, Séverine Bézie, Lorena Usero, ..., Karine Bernardeau, Stéphanie Gras, Carole Guillonneau

Correspondence

carole.guillonneau@univ-nantes.fr

In Brief

Picarda et al. describe MHC class II-derived peptides recognized by cross-reactive CD8$^+$ Tregs instrumental for tolerance induction in transplantation between an incompatible donor and recipient.

Highlights

- Human and rat CD8$^+$ Tregs recognize long peptides derived from donor MHC class II molecules
- A cross-reactive CD8$^+$ Treg population recognizes different MHC class II-derived peptides
- *In vivo* tolerogenic peptide vaccination induces CD8$^+$ Tregs and transplantation tolerance

Data Resources

6NF7

Picarda et al., 2019, Cell Reports *29*, 4245–4255
December 24, 2019
https://doi.org/10.1016/j.celrep.2019.11.106

CellPress

Cell Reports
Report

Cross-Reactive Donor-Specific CD8$^+$ Tregs Efficiently Prevent Transplant Rejection

Elodie Picarda,[1,2,7] Séverine Bézie,[1,2] Lorena Usero,[1,2] Jason Ossart,[1,2] Marine Besnard,[1,2] Hanim Halim,[4] Klara Echasserieau,[3] Claire Usal,[1,2] Jamie Rossjohn,[4,5,6] Karine Bernardeau,[3] Stéphanie Gras,[4,5] and Carole Guillonneau[1,2,8,*]

[1]Nantes Université, INSERM, Centre de Recherche en Transplantation et Immunologie, UMR 1064, ITUN, 44000 Nantes, France
[2]LabEx IGO "Immunotherapy, Graft, Oncology," Nantes, France
[3]Plateforme de protéines recombinantes P2R IFR26, CRCNA-UMR892 INSERM, Nantes, France
[4]Infection and Immunity Program and Department of Biochemistry and Molecular Biology, Biomedicine Discovery Institute, Monash University, Clayton, VIC 3800, Australia
[5]ARC Centre of Excellence in Advanced Molecular Imaging, Monash University, Clayton, VIC 3800, Australia
[6]Institute of Infection and Immunity, School of Medicine, Cardiff University, Cardiff CF14 4XN, UK
[7]Present address: Department of Microbiology and Immunology, Albert Einstein College of Medicine, Bronx, NY 10461, USA
[8]Lead Contact
*Correspondence: carole.guillonneau@univ-nantes.fr
https://doi.org/10.1016/j.celrep.2019.11.106

SUMMARY

To reduce the use of non-specific immunosuppressive drugs detrimental to transplant patient health, therapies in development aim to achieve antigen-specific tolerance by promoting antigen-specific regulatory T cells (Tregs). However, identification of the natural antigens recognized by Tregs and the contribution of their dominance in transplantation has been challenging. We identify epitopes derived from distinct major histocompatibility complex (MHC) class II molecules, sharing a 7-amino acid consensus sequence positioned in a central mobile section in complex with MHC class I, recognized by cross-reactive CD8$^+$ Tregs, enriched in the graft. Antigen-specific CD8$^+$ Tregs can be induced *in vivo* with a 16-amino acid-long peptide to trigger transplant tolerance. Peptides derived from human HLA class II molecules, harboring the rat consensus sequence, also activate and expand human CD8$^+$ Tregs, suggesting its potential in human transplantation. Altogether, this work should facilitate the development of therapies with peptide epitopes for transplantation and improve our understanding of CD8$^+$ Treg recognition.

INTRODUCTION

The therapeutic tolerogenic potential of regulatory T cells (Tregs) has been highlighted by recent studies in numerous fields, including transplantation, and several clinical trials using polyclonal Tregs have started (Fuchs et al., 2018; Tang and Vincenti, 2017). However, it has been shown that antigen-specific Tregs (both CD4$^+$ and CD8$^+$) have greater potential than unspecific polyclonal Tregs to control graft rejection and even induce tolerance (Flippe et al., 2019; Masteller et al., 2006; Picarda et al., 2011, 2014; Sagoo et al., 2011; Bézie et al., 2019). Thus, antigen therapy appears to be a promising donor-specific therapeutic for the prevention of transplant rejection, which could diminish or even replace the non-specific immunosuppressive drugs that are so deleterious for the patient health in the long term (Marcén, 2009; Meier-Kriesche et al., 2006; Picarda et al., 2011, 2014). However, principles for the design and choice of donor-derived peptides to induce immunoregulation are unknown, and donor-derived peptides recognized by CD4$^+$ and CD8$^+$ Tregs have not been identified in human transplantation. So far, donor blood transfusion protocols in animal models have resulted in highly efficient donor-specific tolerance induction in a CD8- or CD4-dependent manner (Douillard et al., 1999; Liu et al., 2004; Ueta et al., 2018; Vignes et al., 2000), but they are not clinically applicable and could trigger global alloresponses. Using libraries of donor-derived peptides, we previously identified in a rat model of tolerance the sequence of a dominant peptide derived from a donor major histocompatibility complex (MHC) class II (RT1.D^u) molecule and presented by a MHC class I (RT1.A^a) molecule that specifically triggered activation of CD8$^+$ Tregs (Picarda et al., 2014). Despite being less studied than CD4$^+$ Tregs (Bézie et al., 2018a), CD8$^+$ Tregs can efficiently inhibit transplant rejection in rat models of cardiac transplantation (Bézie et al., 2015a; Guillonneau et al., 2007; Picarda et al., 2017) and in humanized non-obese diabetic (NOD)-severe combined immunodeficiency (SCID)-Il2r$\gamma^{-/-}$ (NSG) mouse models of human skin transplantation and xenogeneic graft versus host disease (GVHD) (Bézie et al., 2018b). We showed that immune therapy using this peptide alone efficiently inhibited fully incompatible cardiac allograft rejection in rat through direct induction of T cell receptor (TCR) Vβ11 skewed CD8$^+$ Tregs (Picarda et al., 2014). Recently, the structure of a human-induced CD4$^+$ Treg TCR was solved in complex with a proinsulin-derived peptide presented by a MHC class II molecule and demonstrated a 180° polarity reversal, challenging our understanding of TCR recognition (Beringer et al., 2015).

In this study, we identified and characterized MHC class II-derived peptides sharing a consensus motif in rat and human, forming a unique structural complex with MHC class I, and

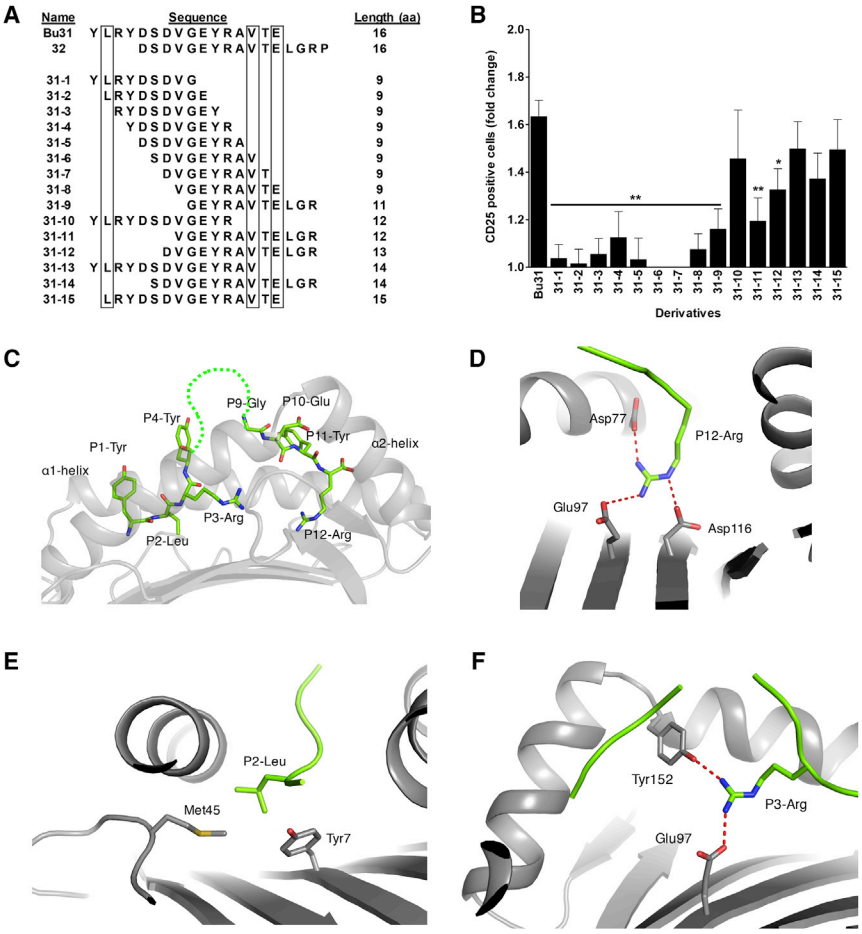

Figure 1. Donor-Derived Bu31 Peptide and Its Longest Derivatives Activate CD8$^+$ Treg Function and Crystallize in Complex with Self-MHC Class I Molecule

CD8$^+$ Tregs were cocultured for 6 days with syngeneic CpG-matured pDCs in the presence of peptides.

(A) Sequence and length of 15 Bu31 derivatives. Boxes highlight mismatched aa between donor and recipient.

(B) Treg activation in response to Bu31 derivatives was analyzed by CD25 expression. Bars represent the ratio between the percentage of CD25-positive cells after peptide stimulation and the percentage of CD25-positive cells in the control condition without peptide ± SEM. Mann-Whitney test, *$p < 0.05$, **$p < 0.01$ versus Bu31 condition. n = 3 to 14 for each peptide.

(C) Structure of the RT1.A^a/Bu31-10 complex.

(D–F) Zoomed-in views of the Bu31-10 peptide, showing interactions between the RT1.A^a molecule and the P12-Arg (D), P2-Leu (E), and P3-Arg (F) anchor residues of the peptide, respectively. Peptide is in green and MHC is in gray; red dashed lines represent hydrogen bonds formed between peptide and MHC.

activating cross-reactive CD8$^+$ Treg function *in vitro* and *in vivo* upon vaccination, which induced graft tolerance. These findings improve our understanding of antigen presentation and specificity to Tregs and could facilitate the development of therapies with peptide epitopes for transplantation.

RESULTS

A Self-MHC Class I Molecule Accommodates Long Peptide from a Donor MHC Class II Molecule with a Mobile Central Section Necessary to Activate CD8$^+$ Treg Function

We previously described a library of 16 amino acid (aa)-long overlapping peptides generated from polymorphic domains of the donor MHC molecules of LEW.1W rats (Picarda et al., 2014). We showed that peptide 51 (further called Du51, sequence NREEYARFDSDVGEYR derived from the β1 domain of the β chain of donor MHC class II RT1.D^u) and peptide 31 (further called Bu31, sequence YLRYDSDVGEYRAVTE derived from the β1 domain of the β chain of donor MHC class II RT1.B^u) induced highly significant upregulation of CD25 expression at the cell surface of CD8$^+$CD45RC^{low} Tregs isolated from a tolerant grafted recipient (treated at day 0 with CD40Ig, a chimeric molecule blocking the CD40-CD40L pathway) after 6 days of culture in the presence of matured syngeneic plasmacytoid dendritic cells (pDCs) (Picarda et al., 2014) (Figure S1A). Both peptides shared an 8 aa motif (DSDVGEYR) that is potentially recognized by CD8$^+$ Tregs.

To determine the sequence of the natural donor Bu31 peptide recognized by antigen-specific CD8$^+$ Tregs, we designed a library of 9- to 15-mer degenerated peptides derived from 16-mer Bu31 and 32 peptides (labeled 31-1 to 31-15) (Figure 1A), taking into account the preferential presence of arginine (R) at the C terminus for binding to the MHC class I RT1.A^a molecule (Powis et al., 1996; Stevens et al., 1998a, 1998b; Thorpe et al., 1995). The library was tested in the same *in vitro* assay described earlier. Although none of the 9-mer derivative peptides 31-1 to 31-8 activated CD8$^+$ Tregs, four longer derivatives—31-10, 31-13, 31-14, and 31-15—induced strong CD25 upregulation to a similar level than did Bu31 peptide. Interestingly, they all shared the 7 aa motif SDVGEYR, also present in the previously described Du51 peptide (sequence NREEYARFDSDVGEYR) (Picarda et al., 2014).

We refolded the RT1.A^a molecule in complex with 16-mer Du51 peptide (NREEYARFDSDVGEYR) and Bu31 peptide (YLRYDSDVGEYRAVTE) and overlapping 12-mer Bu31-10 peptide (YLRYDSDVGEYR) and then assessed the stability of each complex using a thermal stability assay. We observed markedly different levels of thermostability among the three peptides: the highest stability was exhibited by the shorter Bu31-10 peptide, with a thermal melting (denaturation) temperature of ~62°C, which was ~12°C higher than either one of the two 16-mer peptides in complex with RT1.A^a (Table S1). Interestingly, the 12-mer

Bu31-10 peptide shares the same P2-Leu and PΩ-Arg residues as 16-mer Bu31 and Du51 peptides, respectively.

Next, we solved the structure of the RT1.A^a molecule in complex with the most stable Bu31-10 peptide at a resolution of 2.9 Å (PDB: 6NF7) (Table S2). The RT1.A^a-Bu31-10 complex crystallized in the $P2_1$ space group, with five peptide-MHC (pMHC) complexes in the asymmetric unit. Each of the five pMHC molecules showed an overall similar antigen-binding cleft conformation (root-mean-square deviation [RMSD] of 0.3 Å). The peptide exhibited a highly mobile conformation (Figure 1C) in the five complexes (RMSD of 0.5–0.9 Å), with weak electron density for the central part of the peptide that was not visible in the electron density (P5-DSDV-P8) (Figure S1B). Similar to previously solved structures of peptide-RT1.A^a complexes, the RT1.A^a-Bu31-10 complex showed a preferred small hydrophobic residue at P2 (Leu/Pro), a larger half-buried P3 residue (Arg/Phe), and a PΩ-Arg (Rudolph et al., 2002; Speir et al., 2001). The two anchor residues at P2 and PΩ are shared with the less stable 16-mer Du51 and Bu31 peptides. The PΩ-Arg of Bu31-10 peptide forms a salt bridge with Asp116, Glu97, and Asp77 of the F pocket within the antigen-binding cleft (Figure 1D). Meanwhile, Bu31 peptide has a PΩ-Glu that is unfavorable in the negatively charged F pocket of RT1.A^a, which may explain the decreased stability of Bu31 peptide compared with Bu31-10 peptide (Table S1). The P2-Leu of Bu31-10 peptide sits above Tyr7 and Met45 of RT1.A^a (Figure 1E); a larger residue such as the P2-Arg of Du51 peptide might lead to steric clashes within the B pocket of the RT1.A^a, which would be unfavorable. This might explain the lower stability of Du51 peptide compared with Bu31-10 peptide. Finally, the P3-Arg of Bu31-10 peptide, which is also shared with Bu31 peptide, formed a salt bridge with Glu97 and a hydrogen bond with Tyr152, further stabilizing the peptide within the RT1.A^a molecule (Figure 1F). Collectively, our data show that the higher stability of Bu31-10 peptide results from favored anchor residues at positions P2, P3, and PΩ that were partially missing within Bu31 or Du51 peptides. In addition, the structure of Bu31-10 peptide in complex with RT1.A^a reveals a mobile central section of the peptide that might be stabilized upon TCR ligation and thus confirms the importance of the consensus sequence SDVGEYR present in each peptide.

A Cross-Reactive CD8$^+$ Treg Population Recognizes Peptides Derived from Different MHC Molecules

To further understand the role of this consensus sequence in the mobile section, we generated MHC class I tetramers for RT1.A^a/Bu31-10 (tet Bu31-10) and RT1.A^a/Du51 (tet Du51) and tested specific binding of CD8$^+$CD45RC^{low} Tregs from spleen, graft, and blood of cardiac graft recipients who had been tolerant for >120 days. Both PE- and APC-conjugated tet Bu31-10 or tet Du51 were used to discriminate a true signal from noise as described previously (Picarda et al., 2014). Non-specific binding to a BV421-labeled RT1.A^a/MTF-E (Tet MTF-E) control tetramer was eliminated, together with dead cells (Figure 2A). Around 1.38% of CD8$^+$CD45RC^{low} Tregs in the graft, 0.67% in the spleen, and 0.25% in the blood were specific for Bu31-10 peptide (Figures 2A, left panels, and 2B). This percentage is 3- to 5-fold lower than the one of dominant Du51-specific cells (Figures 2A, middle panels, and 2B) (Picarda et al., 2014). Analysis of potential Treg cross-reactivity showed that all Bu31-10-specific Tregs also cross-recognized peptide Du51 but a fraction of Du51-specific Tregs did not bind to tet Bu31-10 (Figures 2A, right panels, and 2B). Cross-reactive Tregs were mostly present in the graft, followed by the spleen and to a lesser extent the blood. Moreover, we showed that 20% to 40% of Du51 and Bu31-10 antigen-specific Tregs express FoxP3 (Figure 2C).

Given the non-canonical length of the peptide and the presence of the consensus sequence recognized by both Du51 and Bu31-10 antigen-specific Tregs, we next performed alanine scanning mutagenesis of the Du51 dominant peptide to determine the contribution of each residue to CD8$^+$ Treg recognition and activation (Figure 2D). All alanine analogs showed a substantial reduction in Treg activation compared with wild-type peptide. Substitution of P16-Arg (R16A) resulted in the most significant loss of activation, which might result from its critical role in peptide stability. Substitutions at positions P3-Glu, P4-Glu, and P7-Arg and within the DSDVG peptide motif at P10-Ser and P12-Val also significantly reduced Treg activation, possibly because of peptide instability and defective TCR ligation as suggested by Bu31-10 structural analysis.

Altogether, these results demonstrated that a fraction of CD8$^+$CD45RC^{low} Tregs harbored a flexible TCR capable of recognizing at least two distinct peptides but with a consensus sequence probably key to the recognition.

Stimulation with Bu31 Peptide Leads to Efficient CD8$^+$CD45RC^{low} Treg Activation and Suppressive Function

Given the low frequency of Bu31-specific cells within the total CD8$^+$CD45RC^{low} Treg population, we assessed the capacity of Bu31 peptide to stimulate and increase Treg function after 6 days of incubation with syngeneic pDCs (Figure 2E). Bu31-stimulated CD8$^+$ Tregs upregulated their secretion of interferon gamma (IFNγ), an important cytokine for CD8$^+$ Treg function (Guillonneau et al., 2007), as measured in the culture supernatant (Figure 2E) and their expression of CD25 and CD71 as measured by flow cytometry (Figures 2F and S1A). We also observed a trend for an increase in CD28 and MHC class II expression, but no change in Foxp3 level. After 6 days of Bu31 or control peptide stimulation through the indirect pathway of recognition, CD8$^+$CD45RC^{low} Tregs were recovered and tested for their suppressive capacity in a secondary coculture of effector CD4$^+$CD25$^-$ T cells stimulated by the direct allorecognition pathway with donor pDCs as previously described (Picarda et al., 2014). In this assay, suppression depends on the efficacy of Treg pre-stimulation with peptide and relies on bystander suppression through secretion of inhibitory factors. Bu31-stimulated Tregs significantly suppressed effector T cells proliferation compared with Tregs cultured with a non-activating peptide (Figure 2G). Altogether, we showed Bu31 peptide efficiently activated CD8$^+$CD45RC^{low} Tregs and potentiated their suppressive activity *in vitro*.

In Vivo Tolerogenic Bu31 Peptide Vaccination Induces Tolerance to a Fully Mismatched Cardiac Graft in Rat through CD8$^+$CD45RC^{low} Tregs

To assess the potential of Bu31 peptide in *in vivo* generation of CD8$^+$CD45RC^{low} Tregs and in allograft survival, animals were treated with the peptide as monotherapy at doses of 0.5 or

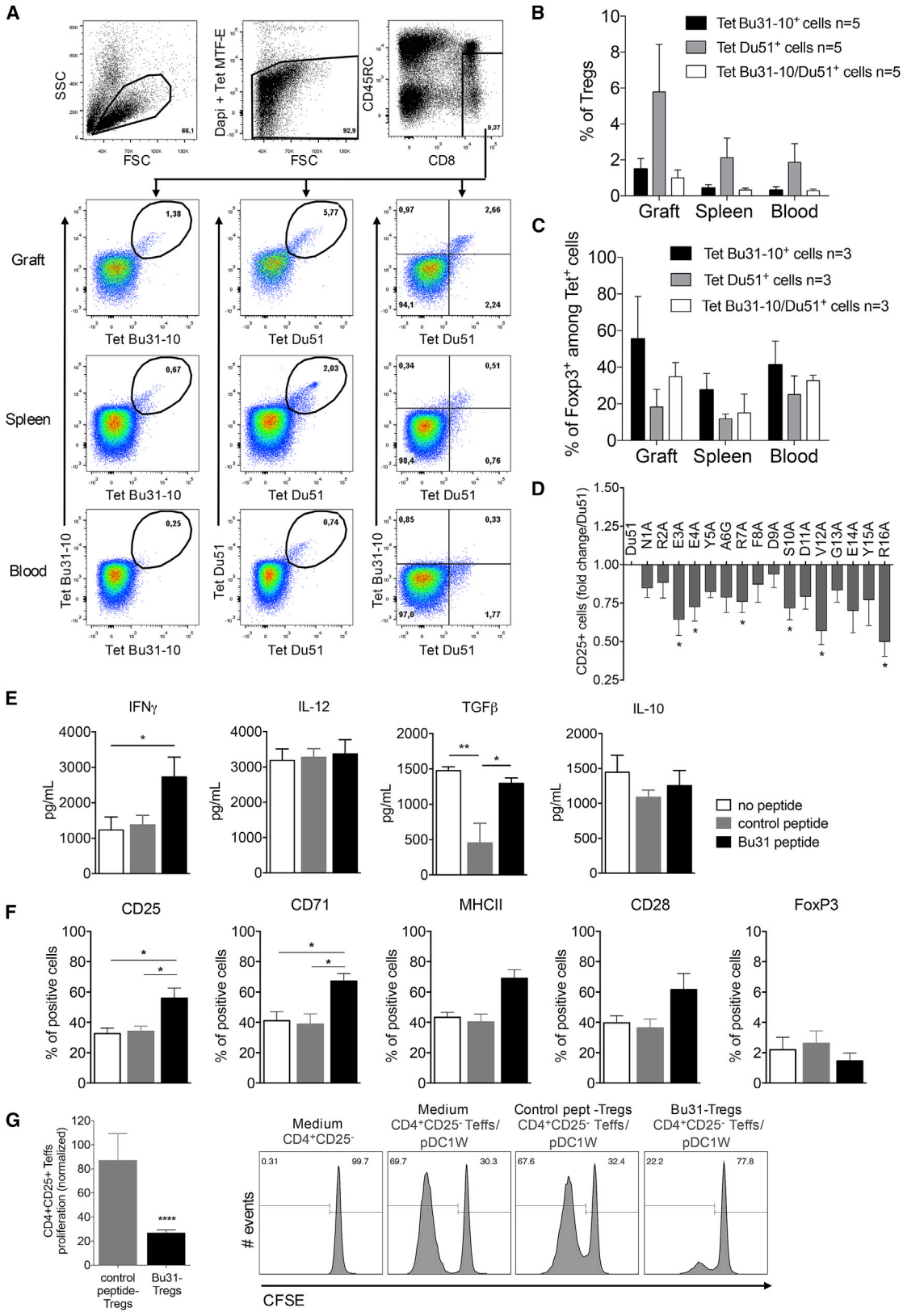

(legend on next page)

1 mg/day for 28 days, starting day 7 before transplantation and constantly released intraperitoneally (i.p.) by mini-osmotic pumps (Figure 3A). Although a dose of 0.5 mg/day was not sufficient to delay cardiac graft rejection, a higher dose of 1 mg/day of peptide induced indefinite allograft survival in 80% of recipients (**$p < 0.01$ compared with 0.5 mg/day and no treatment) (Figure 3B). Long-survival graft induction was donor specific, because third-party Brown Norway (BN) grafts of a different haplotype ($RT1^n$) that did not contain the conserved motif were quickly rejected. In addition, tolerance induced by peptide vaccination depended on $CD8^+$ T cells, because recipients depleted of $CD8^+$ cells using a depleting anti-CD8 monoclonal antibody (mAb) (OX8 clone) (Bézie et al., 2015b; Guillonneau et al., 2007) also rapidly rejected their graft. Histologic analysis of the cardiac graft at day 120 following transplantation showed no signs of chronic rejection (Figure 3C) according to a score previously established (Bézie et al., 2015a; Guillonneau et al., 2007; Picarda et al., 2017). Furthermore, anti-donor humoral responses were abrogated in long-term Bu31-treated recipients (Figure 3D). Finally, we analyzed the suppressive capacity of $CD8^+CD45RC^{low}$ Tregs from long-surviving tolerant recipients *in vitro* in the presence of effector $CD4^+CD25^-$ T cells and donor pDCs (Figure 3E) and *in vivo* upon adoptive transfer in newly grafted irradiated recipients (Figure 3F). Tregs from Bu31-treated recipients were significantly more suppressive than naive cells (Figure 3E), with an almost total inhibition of effector $CD4^+$ T cell proliferation at 1:4 and 1:2 effector:suppressor ratios. *In vivo*, adoptive cell transfer of either total splenocytes or $CD8^+CD45RC^{low}$ Tregs from long-term tolerant Bu31-treated rats significantly delayed allograft rejection in secondary transplanted recipients compared with naive splenocytes (Figure 3F).

Overall, these results demonstrated that short-term tolerogenic vaccination starting before transplantation efficiently induced tolerance, inhibited cellular and antibody-mediated rejection, and improved $CD8^+CD45RC^{low}$ Treg suppressive function.

16 aa Human MHC Class II-Derived Peptides Bearing the Conserved SDVGE-X-R Motif Activate Human $CD8^+CD45RC^{low}$ Tregs

To better understand the relevance of our findings in human transplantation, we designed four 16 aa peptides from four random human histocompatibily leucocyte antigen (HLA) class II alleles based on their alignment with sequences of the rat Du51 peptide (NREEYARFDSDVGEYR) and the overlapping 12-mer Bu31-10 peptide (YLRYDSDVGEYR), both bearing the SDVGEYR motif at the C-terminal end (Figure 4A). We individually tested these human peptides differing at position 2, 5, 6, 14, or 15 in a 5-day culture assay using $CD8^+CD45RC^{low}$ Tregs and autologous pDCs from the same individuals in the presence of interleukin (IL)-2 and CpG in serum-free Texmacs medium (Figure 4A). CD25 and CD69 expression was upregulated on Tregs following incubation with Hpep1, Hpep2, and Hpep4 peptides and reached statistical significance for Hpep2 (Figure 4B). These three peptides share the conserved SDVGE-X-R 7 aa motif; Hpep3 has a valine (V) in place of the glutamic acid (E) at p14 of the peptide, probably affecting TCR recognition. To determine whether Tregs could be expanded using such HLA class II-derived peptide, we set up an expansion protocol using sorted $CD8^+$ Tregs and APCs from the same individual with the Hpep2 peptide in the presence of IL-2, IL-15, and CpG and compared the results with those of a polyclonal stimulation (anti-CD3/CD28 mAbs) (Bézie et al., 2018b) (Figure 4C). Hpep2 stimulation resulted in 8-fold expansion of total $CD8^+$ Tregs in 14 days, although actual expansion of the small Hpep2-specific Treg fraction present at day 0 may be much higher (Figure 4D). Importantly, both Hpep2- and anti-CD3/CD28 mAb-stimulated Tregs retained their capacity to suppress an allogeneic immune response after expansion, similar to fresh $CD8^+$ Tregs (Figure 4E). Peptide-stimulated Tregs tend to be more suppressive than polyclonal Tregs, suggesting the potential benefit of expanding antigen-specific Tregs for therapy. We did not observe significant differences in the level of expression of Foxp3, GITR, IL-10, IFNγ, and IL-34 in Hpep2 or anti-CD3/28 expanded $CD8^+$ Tregs (Figure S2).

Altogether, HLA class II-derived peptides bearing the consensus SDVGE-X-R 7 aa motif efficiently activated and expanded suppressive human $CD8^+CD45RC^{low}$ Tregs.

DISCUSSION

Understanding antigen presentation, recognition, and subsequent Treg activation and expansion is crucial for the development of therapeutic strategies for the treatment of numerous

Figure 2. A Cross-Reactive $CD8^+$ Treg Population Recognizes Distinct Donor Peptides Sharing a Consensus Sequence with Key Residues Necessary for Activation and Efficient Suppressive Function

(A and B) More than 120 days after cardiac transplantation and CD40Ig treatment, dual Tet Bu31-10 and Tet Du51 staining was performed *ex vivo* in five independent experiments on graft, spleen, and blood from tolerant recipients. Percentages of $tetramer^+$ cells are shown after gating on live cells ($DAPI^-$), Tet MTF-E^- (irrelevant tetramer), and $CD8^+CD45RC^{low}$ cells. One representative staining (A) and mean ± SEM (B) are shown.

(C) Percentage of $Foxp3^+$ cells among $Bu31\text{-}10^+$, $Du51^+$, and Bu31-10/Du51 double-positive $CD8^+CD45RC^{low}$ Tregs from graft, spleen, and blood. Graphs represent mean ± SEM.

(D) Treg activation induced by native Du51 and a panel of single amino acid alanine analogs (indicated as N1A to R16A for each position in the Du51 sequence) after 6 days of coculture with syngeneic CpG-matured pDCs. Bars represent the fold change of CD25 activation compared with Du51 dominant peptide ± SEM. *$p < 0.05$ versus Du51, n = 6 for each peptide.

(E and F) Fresh $CD8^+$ Tregs and syngeneic CpG-matured pDCs were cultured for 6 days, alone, with a control peptide or with Bu31 peptide. Expression of indicated markers was analyzed in the culture supernatant by ELISA (E) or on $CD8^+$ Tregs by flow cytometry (F) after *in vitro* stimulation. Graphs represent mean ± SEM. Mann-Whitney test, *$p < 0.05$, **$p < 0.01$, n = 4 to 7.

(G) At day 6, Tregs were isolated by cell sorting (TCR^+), and their capacity to suppress MLR assay was analyzed. The relative proportion of naive CFSE-labeled dividing LEW.1A $CD4^+CD25^-$ T cells after stimulation with donor LEW.1W pDCs was analyzed at day 6 of culture, in the absence or presence of 6 days of peptide-stimulated $CD8^+$ Tregs at a 1:1 ratio of effector:suppressor. On the left, the graph represents mean ± SEM. n = 4. One sample t test versus 100% proliferation, ****$p < 0.0001$. On the right, representative histograms are shown.

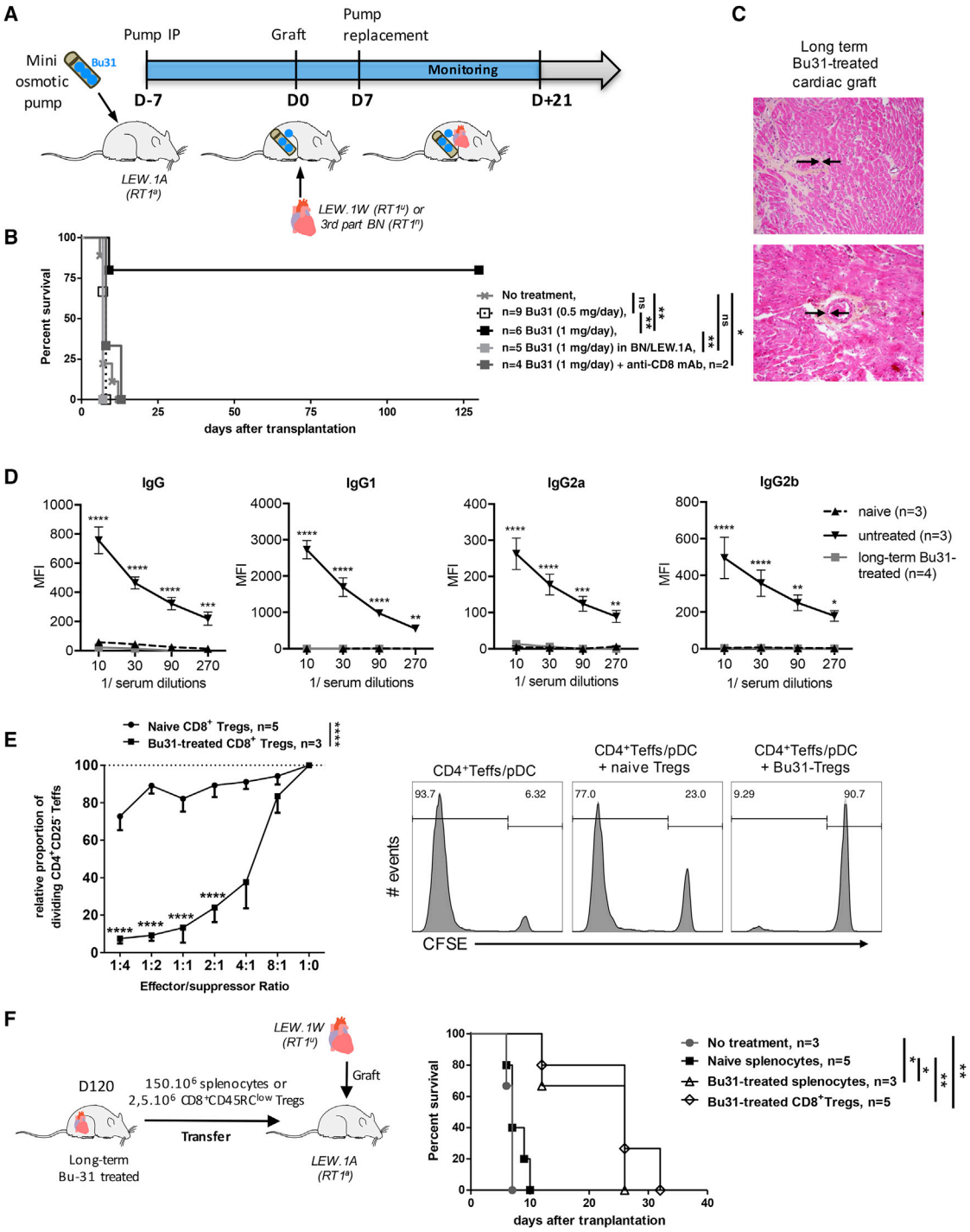

Figure 3. Tolerogenic Vaccination with Bu31 Peptide Induces Allograft Tolerance through Potentiation of Specific CD8$^+$ Tregs' Suppressive Activity

(A) Tolerogenic vaccination protocol with mini-osmotic pump implantation in the abdomen of cardiac allograft recipient from day 7 before transplantation to day 21 post transplantation.

(B) Recipients were either untreated (n = 9) or treated with short-term continuous peptide infusion by i.p. mini-osmotic pumps delivering either 0.5 mg/day (n = 6) or 1 mg/day (n = 5) of Bu31 peptide alone or combined with a depleting anti-CD8α mAb (OX8) (n = 2) or 1 mg/day in the BN/LEW.1A strain combination (n = 4). Log rank test, *p < 0.05, **p < 0.01.

(C) Representative H&E histology of two representative sections of cardiac graft from long-surviving Bu31-treated rats at day 120 post-transplantation and treatment. Arrows indicate the intimal wall of the vessels. Original magnification, ×100.

(legend continued on next page)

diseases, such as transplant rejection and auto-immunity. We previously demonstrated that a 16-mer-long dominant peptide derived from a donor MHC class II molecule strongly activated $CD8^+$ Tregs (Picarda et al., 2014), contrasting with literature describing a more common short length preference for MHC class I. In the present study, we made a similar observation with a peptide derived from a different MHC class II molecule (16 aa original sequence and not less than a derivative of 12 aa). Historically, studies of random peptide libraries and of mass spectrometry have been limited to short lengths of 8 to 10 aa and have allowed the development of powerful tools for prediction of potential antigenic epitopes but rarely exceeded 11 aa. However, about 10% of presented peptides have a length greater than 11 aa (Burrows et al., 2006), even up to 25 aa (Bell et al., 2009). Recent studies suggest that MHC class I can accommodate peptides much longer than previously established, inviting broadening studies and peptide binding algorithms up to 15/16 aa. This clear preference for long peptides from two distinct MHC molecules observed for $CD8^+$ Tregs is intriguing, and it would be interesting to know whether this is a general feature of $CD8^+$ Tregs. Rist and colleagues demonstrated that HLA polymorphism affects the length of peptide presentation and $CD8^+$ T cell response (Rist et al., 2013). It is not clear yet whether our finding regarding the characteristic of structural presentation is restricted to $RT1.A^a$ MHC class I presentation, known to accommodate long peptides (Stevens et al., 1998b), or whether it applies to other haplotypes in rat and human, as suggested by our results using long peptides in the human setting. Binding of long peptides on MHC class I has been shown in the same rat strain for a minor antigen peptide of 13 aa called MTF-E, and the structure revealed two conformations of the peptide, which forms a large and flexible bulge out of the MHC cleft (Speir et al., 2001), suggesting a high level of peptide flexibility that can be observed for long peptides in complex with MHC class I molecules (Chan et al., 2018; Ebert et al., 2009; Hassan et al., 2015; Josephs et al., 2017). Peptide length, and perhaps flexibility, might be important for $CD8^+$ Treg recognition, because no peptide variant shorter than 15 aa for the $RT1.D^u$ and 12 aa for the $RT1.B^u$ chains could efficiently activate $CD8^+$ Tregs. In addition, usage of different anchor residues for the three peptides analyzed seems greater than what has been commonly described for T cell epitopes (Powis et al., 1996; Stevens et al., 1998a; Thorpe et al., 1995). In a tumor model, two distinct polyclonal TCRs recognizing a HLA class I-restricted dominant tumor epitope adopted differing TCR recognition modes, suggesting that extensive flexibility at the TCR-pMHC class I interface engenders recognition (Chan et al., 2018). An interesting feature of the different peptides we studied was the presence of a common motif DSDVGEYR, allowing recognition by a common pool of cross-reactive Tregs. Tetramer staining revealed that Bu31-10-specific $CD8^+$ Tregs also recognized the Du51 peptide, suggesting either flexibility of the TCR recognition or focused recognition on the shared peptide motif. We previously showed that Du51-specific Tregs' TCR was biased toward the Vβ11 family, suggesting that this may also be the case for Bu31-specific Tregs (Guillonneau et al., 2007; Picarda et al., 2014). We confirmed that the two allopeptides involved in acute rejection in the same mismatched cardiac allograft model did not activate $CD8^+$ Tregs and that effector T cells isolated from rejecting untreated animals did not recognized the tolerogenic peptides (Ballet et al., 2009; Picarda et al., 2014).

The use of a soluble peptide as a therapeutic to decrease transplant rejection and selectively induce tolerance through antigen-specific Tregs was both feasible and efficient in our model. Although these Tregs were capable of potent bystander suppression *in vitro*, they did not prevent third-party allograft rejection *in vivo*, possibly because of a lower Treg:Teff ratio *in vivo*, stronger alloresponse to the third-party antigens, and the role played by innate immunity and B cells in rejection. Future work is needed to assess the detailed mechanism of tolerance induction *in vivo* and better understand the potential of bystander suppression mediated by antigen-specific Tregs and the roles played by IFNγ, transforming growth factor β (TGF-β), and IL-34. Although others have shown pMHC multimers can efficiently inhibit autoimmune diseases (Masteller et al., 2003), administration of tolerogenic pMHC multimers induced Treg apoptosis and graft rejection in our model (data not shown), suggesting a high avidity of the TCR for these tolerogenic multimers resulting in strong activation-induced cell death and the requirement for low-antigen doses in the context of transplantation (Mallone et al., 2004; Oling et al., 2010). Several studies have demonstrated the immunomodulatory effect of synthetic peptides derived from conserved regions of MHC molecules on alloimmune responses (Zang and Murphy, 2005): *in vitro* by inhibition of cell-cycle progression (Boytim et al., 1998) or induction of apoptosis (Murphy et al., 1999) and *in vivo* by inhibiting activation and effector function of allogeneic T cells in a mouse model of donor-specific transfusion (Murphy et al., 2003). In addition, administration of a peptide derived from the HLA-B7 molecule named Allotrap and associated with cyclosporine prolonged skin allograft survival in mice (Buelow et al., 1995) and heart allograft survival in rats while attenuating arteriosclerosis (Murphy et al., 1997). In mice, intratracheal administration of a 15-mer derived from the hypervariable region of H2-Kb prolonged cardiac allograft survival

(D) Immunoglobulin G (IgG), IgG1, IgG2a, or IgG2b alloantibody production in naive (n = 3), untreated (n = 3), or Bu31-treated (n = 4) animals > 120 days after transplantation. Graphs represent MFI ± SEM. Two-way ANOVA test, Bonferroni post-test, *p < 0.05, **p < 0.01, ***p < 0.001, ****p < 0.0001.

(E) *In vitro* $CD8^+$ Treg suppressive activity from naive or Bu31-treated cardiac allograft recipients following cell sorting > 120 days after transplantation. Naive (n = 5) or Bu31-$CD8^+$ (n = 3) Tregs, CFSE-labeled $CD4^+CD25^-$ effector T cells, and allogeneic pDCs were cocultured for 6 days. Proliferation of $CD4^+CD25^-$ T cells in the control condition with pDCs and without Tregs (~80%) was given the value 100 in each experiment. On the left, the graph represent mean ± SEM of the relative proportion of dividing $CD4^+$ T cells. Two-way ANOVA test, Bonferroni post-test, ****p < 0.0001. On the right, one representative staining at ratio 1:1 for effector:suppressor is shown.

(F) 120 after transplantation, 150×10^6 total splenocytes or 2.5×10^6 sorted $CD8^+$ Tregs from the spleen of naive or Bu31-treated cardiac allograft recipients were adoptively transferred into naive irradiated LEW.1A recipients transplanted with LEW.1W donor heart. Results are expressed as the percentage of allograft survival as monitored by palpation. Log rank test, *p < 0.05, **p < 0.01.

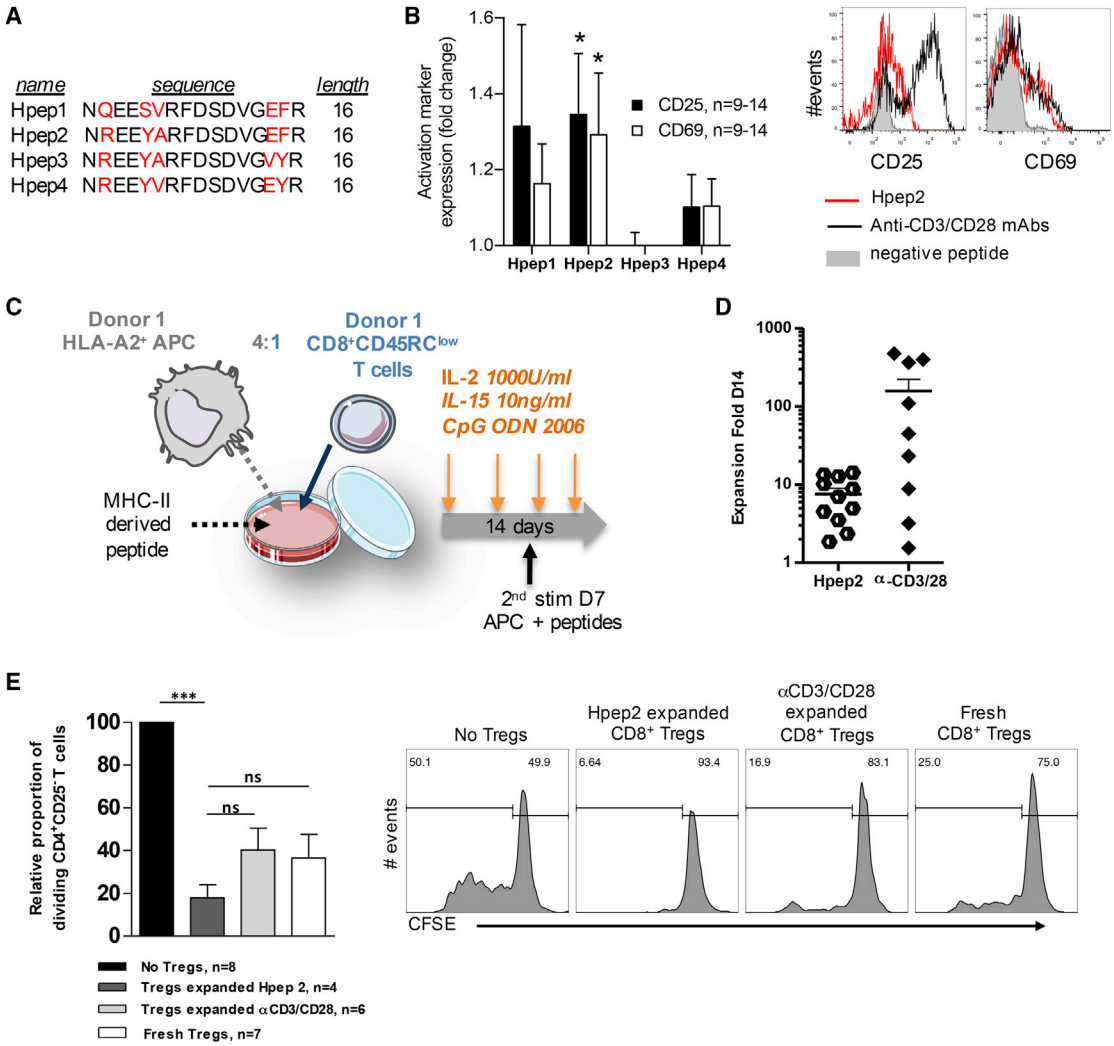

Figure 4. Long MHC Class II Peptides Activate and Expand Human CD8$^+$ Tregs

(A) 16 aa peptides were designed on 4 human MHC class II alleles and tested for CD8$^+$ Treg activation in 5 days of culture with HLA-A2$^+$ syngeneic pDCs in medium supplemented with CpG and IL-2. Peptide mismatches are highlighted in red.

(B) CD8$^+$ Treg activation in response to each peptide was quantified based on CD25 and CD69 expression. Bars ± SEM represent the fold change of positive cells after peptide stimulation compared with the control condition with an irrelevant peptide. Wilcoxon test versus 1, *p < 0.05. n = 9 to 14 for each peptide. Representative histograms are shown on the right.

(C) Protocol of CD8$^+$ Treg expansion by Hpep2 peptide. CD8 Tregs were stimulated at day 0 and day 7 by syngeneic HLA-A2$^+$ APCs, Hpep2 peptide, IL-2, IL-15, and CpG. Cytokines were added twice a week.

(D) Total Treg fold expansion after 14 days of culture with Hpep2 or anti-CD3/anti-CD28 mAbs (versus day 0). Individual samples and mean ± SEM are shown.

(E) After 14 days of peptide or polyclonal stimulation, expanded Tregs were tested for suppressive activity on syngeneic CFSE-labeled CD4$^+$CD25$^-$ T cells stimulated with allogeneic APCs pooled from 3 healthy volunteers, compared with fresh Tregs. Bars ± SEM represent the relative proportion of dividing CD4$^+$CD25$^-$ T cells. ***p < 0.001. n = 2 to 5. Representative histograms are shown on the right.

(Akiyama et al., 2002) or induced tolerance, in combination with a non-depleting anti-human CD4 antibody (Aramaki et al., 2003), and generated regulatory cells. Finally, according to a pilot study in humans, oral administration of low doses of peptides derived from donor MHC (HLA-DR2) molecules to patients with chronic dysfunction of renal allograft induced complete inhibition of indirect alloreactivity *in vitro*, but suppression mechanisms have not been elucidated (Womer et al., 2008). Du51 and Bu31 peptides identified in our model have >90% homology with human HLA-DP, HLA-DQ, and HLA-DR molecules. To emphasize the clinical scope and potential future therapeutic interest of our work, we studied the response of human CD8$^+$ Tregs to these homologous peptides (Bézie et al., 2018b). One peptide in particular bearing the consensus SDVGE-X-R 7 aa motif efficiently activated and expanded CD8$^+$ Tregs. Importantly, Tregs retained their suppressive potential and tolerogenic phenotype after 14 days of expansion, suggesting this peptide specifically expanded Tregs, not effector T cells.

However, expansion remained low compared to polyclonal anti-CD3/CD28 mAb stimulation, although suppressive potential seems to be slightly increased, and future work is needed to optimize growing conditions and obtain sufficient $CD8^+$ Treg numbers for cell therapy.

Altogether, this work improves our understanding of $CD8^+$ Treg recognition and sets the path for development of therapies with peptide epitopes in transplantation.

STAR★METHODS

Detailed methods are provided in the online version of this paper and include the following:

- KEY RESOURCES TABLE
- LEAD CONTACT AND MATERIALS AVAILABILITY
- EXPERIMENTAL MODEL AND SUBJECT DETAILS
  - Animals and cardiac transplantation models
  - Human Samples
- METHOD DETAILS
  - Peptides libraries
  - Cell purification
  - Peptide stimulation assay
  - Suppression assays
  - Extracellular and intracellular stainings
  - Tetramer staining
  - Cytokine assays
  - Peptide therapy *in vivo*
  - Adoptive cell transfer
  - Expansion *in vitro* of human $CD8^+CD45RC^{low}$ Tregs
  - Protein purification and structure determination
  - Thermal stability assay
- QUANTIFICATION AND STATISTICAL ANALYSIS
- DATA AND CODE AVAILABILITY
  - Data Resources

SUPPLEMENTAL INFORMATION

Supplemental Information can be found online at https://doi.org/10.1016/j.celrep.2019.11.106.

ACKNOWLEDGMENTS

We thank Dr. Ignacio Anegon for critical reading of the manuscript. We thank Emmanuel Merieau for technical assistance in animal models and Bernard Martinet for purification of OX8 antibodies. We thank the Monash Macromolecular Crystallization Facility staff for assistance with crystallization and the staff at the Australian synchrotron for assistance with data collection. We thank the Vector Core of the University Hospital of Nantes, which is supported by the Association Française Contre les Myopathies, for producing the adenoviral vectors. We thank the Fondation Progreffe for financial support and Crédit Agricole for the donation of the FACSAria. This work was realized in the context of the Labex IGO program and IHU-Cesti project supported by the National Research Agency via the investment of the future program (ANR-11-LABX-0016-01 and ANR-10-IBHU-005). The IHU-Cesti project is also supported by Nantes Metropole and the Pays de la Loire Region. This work was supported by an ESOT Junior Basic Science Grant, a Marie Curie fellowship from the 6th FP of the EU, and an Etoiles Montantes from Pays de la Loire to C.G. E.P. was supported by an INSERM-Region Pays de la Loire Fellowship, J.O. was supported by the Fondation pour la Recherche Médicale (PLP20141031245), and J.R. is supported by an ARC Laureate Fellowship. S.G. is a Monash Senior Research Fellow.

AUTHOR CONTRIBUTIONS

E.P. contributed to data collection, experimentation, analysis, and writing of the manuscript. S.B., L.U., J.O., H.H., M.B., K.E., C.U., and K.B. contributed to data collection, experimentation, and analysis. J.R. and S.G. solved the crystal structure and contributed to data collection and experimentation. C.G. conceived, financed, and led the project, analyzed the data, and wrote the manuscript.

DECLARATION OF INTERESTS

Patents have been filed based on the results presented in the paper.

Received: December 20, 2018
Revised: October 14, 2019
Accepted: November 25, 2019
Published: December 24, 2019

REFERENCES

Akiyama, Y., Shirasugi, N., Aramaki, O., Matsumoto, K., Shimazu, M., Kitajima, M., Ikeda, Y., and Niimi, M. (2002). Intratracheal delivery of a single major histocompatibility complex class I peptide induced prolonged survival of fully allogeneic cardiac grafts and generated regulatory cells. Hum. Immunol. *63*, 888–892.

Aramaki, O., Shirasugi, N., Akiyama, Y., Takayama, T., Shimazu, M., Kitajima, M., Ikeda, Y., and Niimi, M. (2003). Induction of operational tolerance and generation of regulatory cells after intratracheal delivery of alloantigen combined with nondepleting anti-CD4 monoclonal antibody. Transplantation *76*, 1305–1314.

Ballet, C., Renaudin, K., Degauque, N., Mai, H.L., Boëffard, F., Lair, D., Berthelot, L., Feng, C., Smit, H., Usal, C., et al. (2009). Indirect CD4+ TH1 response, antidonor antibodies and diffuse C4d graft deposits in long-term recipients conditioned by donor antigens priming. Am. J. Transplant. *9*, 697–708.

Bell, M.J., Burrows, J.M., Brennan, R., Miles, J.J., Tellam, J., McCluskey, J., Rossjohn, J., Khanna, R., and Burrows, S.R. (2009). The peptide length specificity of some HLA class I alleles is very broad and includes peptides of up to 25 amino acids in length. Mol. Immunol. *46*, 1911–1917.

Beringer, D.X., Kleijwegt, F.S., Wiede, F., van der Slik, A.R., Loh, K.L., Petersen, J., Dudek, N.L., Duinkerken, G., Laban, S., Joosten, A., et al. (2015). T cell receptor reversed polarity recognition of a self-antigen major histocompatibility complex. Nat. Immunol. *16*, 1153–1161.

Bézie, S., Picarda, E., Ossart, J., Tesson, L., Usal, C., Renaudin, K., Anegon, I., and Guillonneau, C. (2015a). IL-34 is a Treg-specific cytokine and mediates transplant tolerance. J. Clin. Invest. *125*, 3952–3964.

Bézie, S., Picarda, E., Ossart, J., Martinet, B., Anegon, I., and Guillonneau, C. (2015b). Compensatory Regulatory Networks between CD8 T, B, and Myeloid Cells in Organ Transplantation Tolerance. J. Immunol. *195*, 5805–5815.

Bézie, S., Anegon, I., and Guillonneau, C. (2018a). Advances on CD8+ Treg Cells and Their Potential in Transplantation. Transplantation *102*, 1467–1478.

Bézie, S., Charreau, B., Vimond, N., Lasselin, J., Gérard, N., Nerrière-Daguin, V., Bellier-Waast, F., Duteille, F., Anegon, I., Guillonneau, C., et al. (2019). Human CD8+ Tregs expressing a MHC-specific CAR display enhanced suppression of human skin rejection and GVHD in NSG mice. Blood Adv. *3*, 3522–3538.

Bézie, S., Meistermann, D., Boucault, L., Kilens, S., Zoppi, J., Autrusseau, E., Donnart, A., Nerrière-Daguin, V., Bellier-Waast, F., Charpentier, E., et al. (2018b). *Ex Vivo* Expanded Human Non-Cytotoxic $CD8^+CD45RC^{low/-}$ Tregs Efficiently Delay Skin Graft Rejection and GVHD in Humanized Mice. Front. Immunol. *8*, 2014.

Boytim, M.L., Lyu, S.C., Jung, R., Krensky, A.M., and Clayberger, C. (1998). Inhibition of cell cycle progression by a synthetic peptide corresponding to

residues 65–79 of an HLA class II sequence: functional similarities but mechanistic differences with the immunosuppressive drug rapamycin. J. Immunol. *160*, 2215–2222.

Buelow, R., Veyron, P., Clayberger, C., Pouletty, P., and Touraine, J.L. (1995). Prolongation of skin allograft survival in mice following administration of ALLOTRAP. Transplantation *59*, 455–460.

Burrows, S.R., Rossjohn, J., and McCluskey, J. (2006). Have we cut ourselves too short in mapping CTL epitopes? Trends Immunol. *27*, 11–16.

Chan, K.F., Gully, B.S., Gras, S., Beringer, D.X., Kjer-Nielsen, L., Cebon, J., McCluskey, J., Chen, W., and Rossjohn, J. (2018). Divergent T-cell receptor recognition modes of a HLA-I restricted extended tumour-associated peptide. Nat. Commun. *9*, 1026.

DeLano, W.L. (2002). Unraveling hot spots in binding interfaces: progress and challenges. Curr. Opin. Struct. Biol. *12*, 14–20.

Douillard, P., Vignes, C., Josien, R., Chiffoleau, E., Heslan, J.M., Proust, V., Soulillou, J.P., and Cuturi, M.C. (1999). Reassessment of the role of CD8+ T cells in the induction of allograft tolerance by donor-specific blood transfusion. Eur. J. Immunol. *29*, 1919–1924.

Ebert, L.M., Liu, Y.C., Clements, C.S., Robson, N.C., Jackson, H.M., Markby, J.L., Dimopoulos, N., Tan, B.S., Luescher, I.F., Davis, I.D., et al. (2009). A long, naturally presented immunodominant epitope from NY-ESO-1 tumor antigen: implications for cancer vaccine design. Cancer Res. *69*, 1046–1054.

Emsley, P., Lohkamp, B., Scott, W.G., and Cowtan, K. (2010). Features and development of Coot. Acta Crystallogr. D Biol. Crystallogr. *66*, 486–501.

Evans, P.R., and Murshudov, G.N. (2013). How good are my data and what is the resolution? Acta Crystallogr. D Biol. Crystallogr. *69*, 1204–1214.

Flippe, L., Bézie, S., Anegon, I., and Guillonneau, C. (2019). Future prospects for CD8$^+$ regulatory T cells in immune tolerance. Immunol. Rev. Published online October 8, 2019. https://doi.org/10.1111/imr.12812.

Fuchs, A., Gliwiński, M., Grageda, N., Spiering, R., Abbas, A.K., Appel, S., Bacchetta, R., Battaglia, M., Berglund, D., Blazar, B., et al. (2018). Minimum Information about T Regulatory Cells: A Step toward Reproducibility and Standardization. Front. Immunol. *8*, 1844.

Guillonneau, C., Hill, M., Hubert, F.-X., Chiffoleau, E., Hervé, C., Li, X.-L., Heslan, M., Usal, C., Tesson, L., Ménoret, S., et al. (2007). CD40Ig treatment results in allograft acceptance mediated by CD8CD45RC T cells, IFN-gamma, and indoleamine 2,3-dioxygenase. J. Clin. Invest. *117*, 1096–1106.

Guillot, C., Guillonneau, C., Mathieu, P., Gerdes, C.A., Ménoret, S., Braudeau, C., Tesson, L., Renaudin, K., Castro, M.G., Löwenstein, P.R., and Anegon, I. (2002). Prolonged blockade of CD40-CD40 ligand interactions by gene transfer of CD40Ig results in long-term heart allograft survival and donor-specific hyporesponsiveness, but does not prevent chronic rejection. J. Immunol. *168*, 1600–1609.

Hassan, C., Chabrol, E., Jahn, L., Kester, M.G.D., de Ru, A.H., Drijfhout, J.W., Rossjohn, J., Falkenburg, J.H.F., Heemskerk, M.H.M., Gras, S., and van Veelen, P.A. (2015). Naturally processed non-canonical HLA-A*02:01 presented peptides. J. Biol. Chem. *290*, 2593–2603.

Josephs, T.M., Grant, E.J., and Gras, S. (2017). Molecular challenges imposed by MHC-I restricted long epitopes on T cell immunity. Biol. Chem. *398*, 1027–1036.

Kabsch, W. (2010). XDS. Acta Crystallogr. D Biol. Crystallogr. *66*, 125–132.

Liu, J., Liu, Z., Witkowski, P., Vlad, G., Manavalan, J.S., Scotto, L., Kim-Schulze, S., Cortesini, R., Hardy, M.A., and Suciu-Foca, N. (2004). Rat CD8+ FOXP3+ T suppressor cells mediate tolerance to allogeneic heart transplants, inducing PIR-B in APC and rendering the graft invulnerable to rejection. Transpl. Immunol. *13*, 239–247.

Mallone, R., Kochik, S.A., Laughlin, E.M., Gersuk, V.H., Reijonen, H., Kwok, W.W., and Nepom, G.T. (2004). Differential recognition and activation thresholds in human autoreactive GAD-specific T-cells. Diabetes *53*, 971–977.

Marcén, R. (2009). Immunosuppressive drugs in kidney transplantation: impact on patient survival, and incidence of cardiovascular disease, malignancy and infection. Drugs *69*, 2227–2243.

Masteller, E.L., Warner, M.R., Ferlin, W., Judkowski, V., Wilson, D., Glaichenhaus, N., and Bluestone, J.A. (2003). Peptide-MHC class II dimers as therapeutics to modulate antigen-specific T cell responses in autoimmune diabetes. J. Immunol. *171*, 5587–5595.

Masteller, E.L., Tang, Q., and Bluestone, J.A. (2006). Antigen-specific regulatory T cells—*ex vivo* expansion and therapeutic potential. Semin. Immunol. *18*, 103–110.

Meier-Kriesche, H.-U., Li, S., Gruessner, R.W.G., Fung, J.J., Bustami, R.T., Barr, M.L., and Leichtman, A.B. (2006). Immunosuppression: evolution in practice and trends, 1994–2004. Am. J. Transplant. *6*, 1111–1131.

Murphy, B., Kim, K.S., Buelow, R., Sayegh, M.H., and Hancock, W.W. (1997). Synthetic MHC class I peptide prolongs cardiac survival and attenuates transplant arteriosclerosis in the Lewis–>Fischer 344 model of chronic allograft rejection. Transplantation *64*, 14–19.

Murphy, B., Magee, C.C., Alexander, S.I., Waaga, A.M., Snoeck, H.W., Vella, J.P., Carpenter, C.B., and Sayegh, M.H. (1999). Inhibition of allorecognition by a human class II MHC-derived peptide through the induction of apoptosis. J. Clin. Invest. *103*, 859–867.

Murphy, B., Yu, J., Jiao, Q., Lin, M., Chitnis, T., and Sayegh, M.H. (2003). A novel mechanism for the immunomodulatory functions of class II MHC-derived peptides. J. Am. Soc. Nephrol. *14*, 1053–1065.

Oling, V., Geubtner, K., Ilonen, J., and Reijonen, H. (2010). A low antigen dose selectively promotes expansion of high-avidity autoreactive T cells with distinct phenotypic characteristics: a study of human autoreactive CD4+T cells specific for GAD65. Autoimmunity *43*, 573–582.

Picarda, E., Anegon, I., and Guillonneau, C. (2011). T-cell receptor specificity of CD8(+) Tregs in allotransplantation. Immunotherapy *3* (*Suppl*), 35–37.

Picarda, E., Bézie, S., Venturi, V., Echasserieau, K., Mérieau, E., Delhumeau, A., Renaudin, K., Brouard, S., Bernardeau, K., Anegon, I., and Guillonneau, C. (2014). MHC-derived allopeptide activates TCR-biased CD8+ Tregs and suppresses organ rejection. J. Clin. Invest. *124*, 2497–2512.

Picarda, E., Bézie, S., Boucault, L., Autrusseau, E., Kilens, S., Meistermann, D., Martinet, B., Daguin, V., Donnart, A., Charpentier, E., et al. (2017). Transient antibody targeting of CD45RC induces transplant tolerance and potent antigen-specific regulatory T cells. JCI Insight *2*, e90088.

Powis, S.J., Young, L.L., Joly, E., Barker, P.J., Richardson, L., Brandt, R.P., Melief, C.J., Howard, J.C., and Butcher, G.W. (1996). The rat cim effect: TAP allele-dependent changes in a class I MHC anchor motif and evidence against C-terminal trimming of peptides in the ER. Immunity *4*, 159–165.

Read, R.J. (2001). Pushing the boundaries of molecular replacement with maximum likelihood. Acta Crystallogr. D Biol. Crystallogr. *57*, 1373–1382.

Rist, M.J., Theodossis, A., Croft, N.P., Neller, M.A., Welland, A., Chen, Z., Sullivan, L.C., Burrows, J.M., Miles, J.J., Brennan, R.M., et al. (2013). HLA peptide length preferences control CD8+ T cell responses. J. Immunol. *191*, 561–571.

Rudolph, M.G., Stevens, J., Speir, J.A., Trowsdale, J., Butcher, G.W., Joly, E., and Wilson, I.A. (2002). Crystal structures of two rat MHC class Ia (RT1-A) molecules that are associated differentially with peptide transporter alleles TAP-A and TAP-B. J. Mol. Biol. *324*, 975–990.

Sagoo, P., Ali, N., Garg, G., Nestle, F.O., Lechler, R.I., and Lombardi, G. (2011). Human regulatory T cells with alloantigen specificity are more potent inhibitors of alloimmune skin graft damage than polyclonal regulatory T cells. Sci. Transl. Med. *3*, 83ra42.

Smart, O.S., Womack, T.O., Flensburg, C., Keller, P., Paciorek, W., Sharff, A., Vonrhein, C., and Bricogne, G. (2012). Exploiting structure similarity in refinement: automated NCS and target-structure restraints in BUSTER. Acta Crystallogr. D Biol. Crystallogr. *68*, 368–380.

Speir, J.A., Stevens, J., Joly, E., Butcher, G.W., and Wilson, I.A. (2001). Two different, highly exposed, bulged structures for an unusually long peptide bound to rat MHC class I RT1-Aa. Immunity *14*, 81–92.

Stevens, J., Wiesmüller, K.H., Barker, P.J., Walden, P., Butcher, G.W., and Joly, E. (1998a). Efficient generation of major histocompatibility complex class

I-peptide complexes using synthetic peptide libraries. J. Biol. Chem. *273*, 2874–2884.

Stevens, J., Wiesmüller, K.H., Walden, P., and Joly, E. (1998b). Peptide length preferences for rat and mouse MHC class I molecules using random peptide libraries. Eur. J. Immunol. *28*, 1272–1279.

Tang, Q., and Vincenti, F. (2017). Transplant trials with Tregs: perils and promises. J. Clin. Invest. *127*, 2505–2512.

Thorpe, C.J., Moss, D.S., Powis, S.J., Howard, J.C., Butcher, G.W., and Travers, P.J. (1995). An analysis of the antigen binding site of RT1.Aa suggests an allele-specific motif. Immunogenetics *41*, 329–331.

Ueta, H., Kitazawa, Y., Sawanobori, Y., Ueno, T., Ueha, S., Matsushima, K., and Matsuno, K. (2018). Single blood transfusion induces the production of donor-specific alloantibodies and regulatory T cells mainly in the spleen. Int. Immunol. *30*, 53–67.

Vignes, C., Chiffoleau, E., Douillard, P., Josien, R., Pêche, H., Heslan, J.M., Usal, C., Soulillou, J.P., and Cuturi, M.C. (2000). Anti-TCR-specific DNA vaccination demonstrates a role for a CD8+ T cell clone in the induction of allograft tolerance by donor-specific blood transfusion. J. Immunol. *165*, 96–101.

Womer, K.L., Magee, C.C., Najafian, N., Vella, J.P., Milford, E.L., Sayegh, M.H., and Carpenter, C.B. (2008). A pilot study on the immunological effects of oral administration of donor major histocompatibility complex class II peptides in renal transplant recipients. Clin. Transplant. *22*, 754–759.

Zang, W., and Murphy, B. (2005). Peptide-mediated immunosuppression. Am. J. Ther. *12*, 592–599.

STAR★METHODS

KEY RESOURCES TABLE

REAGENT or RESOURCE	SOURCE	IDENTIFIER
Antibodies		
DAPI	Invitrogen	D3571; RRID: AB_2307445
Mouse anti-γδ TCR	European Collection of Authenticated Cell Culture	V45
Mouse anti-CD45RA	European Collection of Authenticated Cell Culture	OX33; RRID: CVCL_J186
Mouse anti-CD161	European Collection of Authenticated Cell Culture	3.2.3
Mouse anti-CD11b/c	European Collection of Authenticated Cell Culture	OX42; RRID: CVCL_J194
Mouse anti-CD45RC-biotin	European Collection of Authenticated Cell Culture	OX22; RRID: CVCL_G685
Streptavidin-PeCy7	BD Biosciences	N/A
Mouse anti-CD8a-PE	European Collection of Authenticated Cell Culture	OX8; RRID: CVCL_J217
Mouse anti-TCRab-a647	European Collection of Authenticated Cell Culture	R73; RRID: CVCL_J772
Mouse anti-CD25-FITC	European Collection of Authenticated Cell Culture	OX39; RRID: CVCL_J191
Mouse anti-TCR	European Collection of Authenticated Cell Culture	R73; RRID: CVCL_J772
Mouse anti-TCR	European Collection of Authenticated Cell Culture	V65
Mouse anti-CD45RA	European Collection of Authenticated Cell Culture	OX33; RRID: CVCL_J186
Mouse anti-CD45R-PE	European Collection of Authenticated Cell Culture	His24
Mouse anti-CD4-APC	European Collection of Authenticated Cell Culture	OX35; RRID:CVCL_J188
Mouse anti-TCR-FITC	European Collection of Authenticated Cell Culture	R73; RRID: CVCL_J772
Mouse anti-CD45RA-FITC	European Collection of Authenticated Cell Culture	OX33; RRID: CVCL_J186
Mouse anti-CD19	BD Biosciences	Cat#555410; HBI19; RRID: AB_395810
Mouse anti-CD14	BD Biosciences	Cat#550376; M5E2; RRID: AB_393647
Mouse anti-CD16	European Collection of Authenticated Cell Culture	3G8
Mouse anti-CD45RC-FITC	IQ-Products	Cat#IQP-117F; clone MT2
Mouse anti-CD8a-PE-Cy7	BD Biosciences	Cat#557746; RPT8; RRID: AB_396852
Mouse anti-Nrp1-PE	BD Biosciences	Cat#565951; RRID: AB_2744361; clone u21-1283
Mouse anti-CD3-PeCy7	BD Biosciences	Cat#560910; RRID: AB_10563409; clone SK7
Mouse anti-CD4-PerCP-Cy5.5	BD Biosciences	Cat#560650; RRID: AB_1727476; RPA-T4
Mouse anti-CD25- APC-Cy7	BD Biosciences	Cat#557753; RRID: AB_396859; M-A251
Mouse anti-TCRαβ-a647	European Collection of Authenticated Cell Culture	R7/3; RRID:CVCL_J772
Mouse anti-CD8a-PeCy7	Thermofisher Scientific	Cat#25-0084-82; OX8; RRID: AB_10548361
Mouse anti-CD4-PeCy7	BD Biosciences	Cat#561578; W3.25; RRID: AB_10715836
Mouse anti-CD45RC-FITC	European Collection of Authenticated Cell Culture	OX22; RRID: CVCL_G685
Mouse anti-CD28-biotin	European Collection of Authenticated Cell Culture	JJ319
Mouse anti-CD71-biotin	European Collection of Authenticated Cell Culture	OX26; RRID: CVCL_J181
Mouse anti-CD25-biotin	European Collection of Authenticated Cell Culture	OX39; RRID: CVCL_J191
Mouse anti-MHCII-biotin	European Collection of Authenticated Cell Culture	OX6; RRID: CVCL_J208
Rat anti-FoxP3-biotin	Thermofisher Scientific	Cat#13-5773; FjK-165; RRID: AB_466671
Streptavidin-PerCP.Cy5.5	BD Biosciences	Cat#551419
Mouse GITR-PE	Miltenyi Biotec	Cat#130-092-895; DT5D3; RRID: AB_871555
Mouse foxp3-APC	BD Biosciences	Cat#560045; 259D/C7; RRID: AB_1645411
Rat IL-10-BV711	BD Biosciences	Cat#564050; JES3-9D7; RRID: AB_2738564
Mouse IL-34-PE	R&D System	Cat#IC5265P; IC5265P; RRID: AB_10640002
Mouse TGFβ1-PECF594	BD Biosciences	Cat#562422; TW4-9E7; RRID: AB_2737614
Mouse IFNγ-PECF594	BD Biosciences	Cat#562392; B27; RRID: AB_11153859
Fixable Viability Dye eF506	ThermoFisher Scientific	Cat#65-0866

(*Continued on next page*)

Continued

REAGENT or RESOURCE	SOURCE	IDENTIFIER
F Block	BD Biosciences	Cat#564220
RT1.Aa/Du51 tetramer	This paper	N/A
RT1.Aa/Bu31-10 tetramer	This paper	N/A
RT1.Aa/MTF-E tetramer	This paper	N/A
Streptavidin-PE	Thermofisher Scientific	Cat#S21388
Streptavidin-APC	Thermofisher Scientific	Cat#S32362
Streptavidin-BV421	Biolegend	Cat#405225
Rat FoxP3-Pacific Blue	eBiosciences	Cat#48-5773-82; FJK-16 s; RRID: AB_494151
Mouse anti-CD28	BD Biosciences	Cat#555726; CD28.2; RRID: AB_396069
Mouse anti-CD3	European Collection of Authenticated Cell Culture	OKT3; RRID:CVCL_2665
Mouse anti-CD3-PE	BD Biosciences	Cat#555340; RRID: AB_395746; clone HIT3a
Bacterial and Virus Strains		
BL21 E. Coli	ATCC	N/A
AdCD40lg	Plateforme de Production de vecteurs viraux, IRS, Nantes	N/A
Chemicals, Peptides, and Recombinant Proteins		
Penicillin Streptomycin	GIBCO	Cat#15140-122
rhIL-2	Proleukin, Novartis	N/A
rhIL-15	Miltenyi Biotec	Cat#103-095-765
Custom peptides	GL Biochem Ltd (China)	N/A
Collagenase D	Sigma Aldrich	Cat#1108882001
Guanidine	Rowe	CG0112
Urea	Sigma Aldrich	U1250-1KG
Tri-HCL	Goldbio	T-400-5
Na-EDTA	Sigma Aldrich	E4884-500G
L-arginine-HCL	Sigma Aldrich	A5131-1KG
Oxidized gluthatione	Sigma Aldrich	G4376-10G
Reduced gluthatione	Goldbio	G-155-500
Bis-Tris-Propane	Sigma Aldrich	B6755-25G
PEG 8000	Sigma Aldrich	202452-500G
Mg2SO4	Sigma Aldrich	M7506-500G
Critical Commercial Assays		
Fix/Perm kit	Ebiosciences	Cat#00-5223-56
IFNg ELISA OptEIA	BD Biosciences	Cat#558861
IL-10 ELISA OptEIA	BD Biosciences	Cat#555134
IL-12 ELISA	ThermoFisher Scientific	Cat#KRC2371
TGFb ELISA	R&D System	Cat#MB100B
Deposited Data		
Crystal structure RT1.Aa/Bu31-10	This paper	PDB: 6NF7
Experimental Models: Cell Lines		
Blood PBMCs	Etablissement Francais du Sang	N/A
Experimental Models: Organisms/Strains		
Rat: LEW.1A	Janvier Labs	N/A
Rat: LEW.1W	Janvier Labs	N/A
Rat: Brown-Norway	Charles River	N/A
CpG 2006	Eurofins Genomics	PTO
CpG ODN 1826	Eurofins Genomics	PTO

(*Continued on next page*)

Continued

REAGENT or RESOURCE	SOURCE	IDENTIFIER
Recombinant DNA		
pET30 vector	Genscript	N/A
Software and Algorithms		
XDS	Kabsch, 2010	http://xds.mpimf-heidelberg.mpg.de/; RRID: SCR_015652
AIMLESS	Evans and Murshudov, 2013	http://www.ccp4.ac.uk/html/aimless.html; RRID: SCR_015747
Phaser program	Read, 2001	http://www.phaser.com/; RRID: SCR_014219
Coot software	Emsley et al., 2010	http://bernhardcl.github.io/coot/; RRID: SCR_014222
Buster program	Smart et al., 2012	https://www.globalphasing.com/buster/; RRID: SCR_015653
Pymol	Schrödinger	https://pymol.org/2/; RRID: SCR_000305
FlowJo X	FlowJo LLC	https://www.flowjo.com/; RRID: SCR_008520
GraphPad Prism 7	GraphPad	https://www.graphpad.com/scientific-software/prism/; RRID: SCR_002798
Other		
PMA	Sigma Aldrich	Cat#P8139
Ionomycin	Sigma Aldrich	Cat#C9272
Brefeldin A	Sigma Aldrich	Cat#B6542
CFSE	Invitrogen	Cat#34554
Ficoll-Paque	Eurobio	Cat#CMSMSL01-01
Mini osmotic pump	Alzet	Cat#2002
Magnetic beads	Dynabeads, Invitrogen	Cat#11033

LEAD CONTACT AND MATERIALS AVAILABILITY

Further information and requests for reagents may be directed to, and will be fulfilled by the corresponding author Carole Guillonneau (carole.guillonneau@univ-nantes.fr).

Tetramers generated in this study will be made available on request but we may require a payment and a completed Materials Transfer Agreement if there is potential for commercial application.

EXPERIMENTAL MODEL AND SUBJECT DETAILS

Animals and cardiac transplantation models

Congenic fully MHC-incompatible LEW.1W (RT1^{u} as donors) and LEW.1A (RT1^{a} as recipients) male rats of 8-12 weeks old were used to perform heterotopic heart allotransplantations as previously described (Guillonneau et al., 2007; Guillot et al., 2002). BN (RT1^{n}) rats were used as 3rd party donors. Allograft long term survival was induced by injection at 3 points into the cardiac ventricular walls of 2.10^{10} infectious particles of adenovirus encoding for extracellular portion of mouse CD40 fused to constant domains of human IgG1 (AdCD40Ig) (Guillonneau et al., 2007; Guillot et al., 2002).

All animal studies were approved by the Pays de la Loire regional French ethics committee for animal care and use.

Human Samples

Blood was collected at the Etablissement Français du Sang (Nantes, France). Heparinized blood samples were taken from healthy volunteers after signing an informed consent approved by the ethical committee of relevant institutions (#N°CPDL-PLER-2018 180). The gender of the donors was not available.

METHOD DETAILS

Peptides libraries

Rat

9 to 15-mer degenerated peptides with aa lagging designed to cover the sequence of parental 16-aa peptides selected and 16-aa peptides with point scan alanine mutations were synthesized by GL Biochem Ltd (China). All aa sequences were confirmed and all

peptides were > 95% homogeneous by analytical reverse phase HPLC. The lyophilized peptides were dissolved in 0.4% sterile DMSO in sterile water and stored at −80°C. Peptides were diluted in complete RMPI-1640 at a concentration of 120μg/ml.

Human

16-aa peptides were randomly designed on human MHC-II alleles based on their alignment with rat sequence (Genscript, USA). Purity was > 90%. Human peptides were dissolved and stored as described above and diluted at 120μg/ml in Texmacs medium for use *in vitro*.

Cell purification

Rat

pDCs, $CD8^+CD45RC^{low}$ T cells and $CD4^+CD25^-$ T cells were purified as previously described (Picarda et al., 2014). Briefly, T cells recovered from spleen following red blood cell lysis were first enriched by negative selection using a mixture of anti-γδ T cell (V65 clone), anti-CD45RA B cell (OX33 clone), anti-CD161 NK cell (3.2.3 clone) and anti-CD11b/c monocyte (OX42 clone) mAbs and magnetic beads (Dynal, Invitrogen). Enriched T cells were then labeled with anti-CD45RC-biotin (OX22 clone) and Strepavidin-PE-Cy7, anti-CD8α–PE (OX8 clone), and for $CD4^+CD25^-$ T cells by adding anti-TCRαβ-Alexa 647 (R73 clone), anti-CD25-FITC (OX39 clone) mAbs and flow-sorted with FACSAria (BD Biosciences). Purity was greater than 98%. For pDCs, splenocytes were digested with collagenase D and enriched for pDCs by negative selection using a mixture of anti-TCR (R73 and V65 clones) T cell, anti-CD45RA (OX33 clone) B cell mAbs and magnetic beads. Enriched cells were then labeled with anti-CD45R-PE (His24 clone), anti-CD4-APC (OX35 clone), anti-TCR-FITC (R73 clone) and anti-CD45RA-FITC (OX33 clone). pDCs were sorted after gating on FITC negative cells, CD45R and CD4 positive cells. Antibodies were obtained from the European Collection of Cell Culture (Salisbury, UK).

Human

PBMCs were isolated by Ficoll-Paque density-gradient centrifugation at 2000 rpm for 20 min at room temperature without brake. Remaining red blood cells and platelets were removed using 5 min incubation with a hypotonic solution and centrifugation at 1000 rpm for 10 min at 4°C. For pDC and T cell sorting, B cells, monocytes and NK cells were magnetically depleted (Dynabeads, Invitrogen) by using anti-CD19 (clone: HBI19, eBiociences), anti-CD14 (clone: M5E2, eBiociences) and anti-CD16 (Clone: 3G8, purified) mAbs respectively. Enriched PBMCs were stained with anti-CD45RC-FITC (clone: MT2, IQ-Products), anti-CD8α-PE-Cy7 (clone: RPT8, eBiociences) and anti-Nrp1-PE (clone: u21-1283, BD Biosciences) for sorting of $CD8\alpha^+CD45RC^{low}$ Tregs and Neuropilin-1^+ pDCs. Enriched PBMCs were stained with anti-CD3-PeCy7 (clone SK7, BD Biosciences), anti-CD4-PerCP-Cy5.5 (clone: RPA-T4, BD Biosciences) and anti-CD25- APC-Cy7 (clone: M-A251, BD Biosciences) mAbs for sorting of $CD4^+CD25^-$ Teff cells. APCs were obtained from PBMCs by either magnetically depleting T cells with an anti-CD3 (OKT3 purified, 5μg/ml) mAb (for stimulation of Teff in proliferation assays) or by gating out T cells during sorting using anti-CD3-PE (clone: HIT3a, BD Biosciences) (for activation and expansion tests). FACS ARIA II (BD biosciences, Mountain View, CA) was used for sorting. Purity was greater than 98%.

Peptide stimulation assay

Rat

1.25×10^4 pDCs from naive LEW.1A rats, 5×10^4 $CD8^+CD45RC^{low}$ Tregs from tolerant > 120 days CD40Ig-treated recipients and 120 μg/ml of individual allogeneic peptides were plated in triplicate in RPMI-1640 medium supplemented with 10% FCS and 0.5μM of CpG ODN 1826 in round-bottom 96 wells plates for 6 days at 37°C, 5% CO2. The CD25 activation marker was then analyzed by flow cytometry.

Human

$CD8^+CD45RC^{low}$ Treg cells and autologous pDCs from the same healthy $HLA\text{-}A2^+$ donor were co-cultured in serum-free Texmacs medium (Miltenyi Biotec) supplemented with IL-2 (25 U/ml, Proleukin, Novartis), CpG ODN 2006 (0.5 μM) and the different synthesized peptides (120 μg/ml) at a ratio 4:1 of Tregs:pDCs for 5 days. $CD8^+CD45RC^{low}$ Treg activation was analyzed based on expression of CD69 and CD25 markers. As negative control and in order to normalize the results, an irrelevant peptide was used (ALIAPV-HAV). Dapi was used as viability marker. As a positive control, $CD8^+CD45RC^{low}$ Tregs were stimulated with anti-CD3 (OKT3, 1 μg/ml) and anti-CD28 mAbs (clone: CD28.2; 1μg/ml). Results were analyzed using the FACS Canto II cytometer (BD Biosciences) and Flowjo software (Tree Star, Inc. USA, version 10).

Suppression assays

Rat

5×10^4 CFSE-labeled $CD4^+CD25^-$ T cells from naive LEW.1A rats and 1.25×10^4 allogeneic pDCs from naive donor LEW.1W animals were plated in triplicate for 6 days in supplemented RPMI-1640 medium in round-bottom 96 wells plates in presence of 5×10^4 facs-sorted $CD8^+CD45RC^{low}$ Tregs from tolerant > 120 days CD40Ig-treated recipients (previously expanded for 6 days with one peptide in presence of pDCs from a naive LEW.1A rats) or from tolerant > 120 days Bu31-treated recipients, or from non-grafted non-treated naive rats.

Proliferation of CFSE-labeled $CD4^+CD25^-$ T cells was analyzed by flow cytometry on FACS Canto II cytometer (BD Biosciences) after gating on DAPI negative TCR^+CD4^+ cells.

Human

CFSE-labeled $CD4^+CD25^-$ Teffs and $CD8^+CD45RC^{low}$ Tregs from the same healthy volunteer ($HLA\text{-}A2^+$) were co-cultured with a pool of allogeneic APCs from 3 different healthy donors ($HLA\text{-}A2^-$) in RPMI1640 medium supplemented with 5% AB serum. Culture was done at 1:1:1 ratio (where 1 = $5x10^4$ cells/well) for 5 days in triplicate in a V-bottom 96 well plate. Proliferation of $CD4^+CD25^-$ responder T cells was analyzed by flow cytometry (FACS Canto II BD Biosciences TM) by gating on $CD3^+CD4^+$ living cells (DAPI negative) and using Flowjo software (Tree Star, Inc. USA, version 10).

Extracellular and intracellular stainings

Rat

For extracellular staining, cells were stained with anti-TCR$\alpha\beta$ (R73, Alexa Fluor 647–conjugated), anti-CD8α (OX8, PE-Cy7-conjugated, Ebiosciences), anti-CD4 (W3.25, PE-Cy7-conjugated), anti-CD45RC (OX22, FITC-conjugated), anti-CD28 (JJ319, biotin- conjugated), anti-CD71 (OX26, biotin- conjugated), anti-CD25 (OX39, biotin-conjugated) and anti-MHC-II (OX6, biotin-conjugated) mAbs. For intracellular staining, cells were permeabilized and stained for Foxp3 (biotin- conjugated, Ebiosciences) using the BD cytofix/cytoperm kit (BD Biosciences) according to the manufacturer's instructions. All biotinylated mAbs were visualized using Streptavidin-PerCP.Cy5.5 (BD Biosciences). Cells were gated by their morphology, DAPI negative viable cells were selected, fluorescence was measured on a FACS Canto II cytometer (BD Biosciences) and data were analyzed using FlowJo software (Tree Star, Inc. USA, version 10).

Human

For the analysis of GITR (clone: DT5D3, Miltenyi Biotec), Foxp3 (clone:259D/C7, BD Biosciences), IL-10 (clone: JES3-9D7, BD Biosciences), IL-34 (clone: IC5265P, R&D), TGFβ1 (clone: TW4-9E7, BD Biosciences) and IFNγ (clone: B27, BD Biosciences), $CD8^+CD45RC^{low}$ Treg cells were stimulated with PMA (50 ng/ml) and ionomycin (1 μg/ml) for 5h in presence of Brefeldin A (10 μg/ml) for the last 4 hours in Texmacs medium (Miltenyi Biotec). In order to select viable cells, Fixable Viability Dye eF506 (ThermoFisher Scientific) was used as viability marker. Fc receptors were blocked before staining (BD Biosciences) and cells were permeabilized with Fix/Perm kit (Ebiociences) for intracellular staining. Cell phenotype was analyzed by flow cytometry using the LSR II (BD Biosciences, Mountain View, CA) and Flowjo software (Tree Star. Inc. USA, version 10).

Tetramer staining

Tetramerizations of $RT1.A^a$/Du51, $RT1.A^a$/Bu31-10 and control $RT1.A^a$/MTF-E (ILFPSSERLISNR) were performed using either streptavidin-PE (Jackson ImmunoResearch) or streptavidin-APC (BD Biosciences) for the first two and streptavidin-BV421 (Biolegend) for the later as previously described (Picarda et al., 2014). Briefly, streptavidin was added at a 4:1-molar monomer:streptavidin ratio, in four equal aliquots added at 15-min intervals at room temperature.

For staining, three tetramers were mixed and added at 10 μg/mL to cells for 1 hour at 4°C. Cells were then stained for CD8 (clone OX8, PECy7) and CD45RC (clone OX22, A488). Cells were then fixed, permeabilized and stained for Foxp3 (Clone FJK-16 s, Pacific Blue) using the BD cytofix/cytoperm kit (BD Biosciences) according to the manufacturer's instructions. Fluorescence was analyzed on a FACS Canto II cytometer (BD Biosciences) after excluding dead cells and non-specific staining.

Cytokine assays

IFNγ and IL-10 were measured in coculture supernatants using ELISA kits from BD Biosciences OptEIA. IL-12 and TGFβ were measured in coculture supernatants using ELISA kit from Invitrogen and R&D System respectively.

Peptide therapy *in vivo*

16-mer Bu31 peptide was dissolved in 0.4% DMSO/PBS and used in mini osmotic pumps (ALZET) implanted intraperitoneally (i.p) in recipients that delivered continuously 0.5 or 1 mg/day for 14 days starting on day −7 before transplantation and replaced at day +7 for another 2 weeks. LEW.1A or third part BN allografts were monitored daily by palpation and allograft rejection was defined as complete cessation of palpable heartbeat. Depleting anti-CD8α mAb (OX8 clone, IgG1) was injected i.p. twice a week at a dose of 3mg/kg starting 7 days before transplantation and until rejection.

Adoptive cell transfer

$150x10^6$ total splenocytes from naive or Bu31-treated tolerant LEW.1A recipients or $2{,}5x10^6$ sorted $CD8^+CD45RC^{low}$ Tregs from the spleen of Bu31-treated tolerant LEW.1A recipients were transferred by i.v. injection into sublethally irradiated (4.5 Gy whole-body irradiation) LEW.1A recipients one day before transplantation.

Expansion *in vitro* of human $CD8^+CD45RC^{low}$ Tregs

$5x10^5$ $CD8^+CD45RC^{low}$ Tregs and $2x10^6$ autologous APCs from $HLA\text{-}A2^+$ healthy donors were seeded in a 24 well plate in Texmacs Medium (Miltenyi Biotec), supplemented with penicillin (100 U/ml), streptomycin (100 μg/ml), rhIL-2 (1000 U/ml, Proleukin, Novartis), rhIL-15 (10ng/ml, Miltenyi Biotec), CpG (0.5 μM), and the different peptides (120 μg/ml) derived from HLA-II molecule (GenScript). As negative control, a negative irrelevant peptide (ALIAPVHAV) was used. As a positive control, $CD8^+CD45RC^{low}$ Tregs were stimulated

with plate-coated anti-CD3 (clone: OKT3, 1 μg/ml) mAb and soluble anti-CD28 mAb (clone: CD28.2; 1 μg/ml). At day 7, Tregs were counted and re-expanded. Cytokines were freshly added twice a week. Finally, at day 14, cells were used for experiments.

Protein purification and structure determination

Heavy chain of RT1.A^a (1–275) and rat β2 m were cloned into pET30 vector for expression in BL21 *Escherichia coli* cells as inclusion bodies. Inclusion bodies were then extracted using several wash buffers, and solubilized in 6 M guanidine. Solubilized inclusion bodies containing RT1.A^a and β2 m, respectively, were used to refold pMHC complexes using the three peptides: Bu31-10 peptide (YLRYDSDVGEYR), Du51 peptide (NREEYARFDSDVGEYR), and Bu31 peptide (YLRYDSDVGEYRAVTE). Refolding was performed in a cold solution (4°C) containing: 3M urea, 10 mM Tris-HCl pH 8, 2 mM Na-EDTA, 400 mM L-arginine-HCl, 0.5 mM oxidized glutathione, and 5 mM reduced glutathione. Each pMHC was then purified using a series of anion exchange chromatography columns.

Crystals of the RT1.A^a/Bu31-10 complex were grown by the vapor-diffusion method in a hanging-drop configuration at 20°C, at a concentration of 10 mg/mL in 0.1 M Bis-Tris-Propane pH 6.6, 28% PEG 8000 and 0.2 M Mg_2SO_4. Crystals were directly flash frozen in liquid nitrogen and data were collected on the MX2 beamline at the Australian Synchrotron, Clayton using the ADSC-Quantum 315r CCD detector (at 100K). Data were processed using XDS (Kabsch, 2010), and AIMLESS software (Evans and Murshudov, 2013) from the CCP4 suite. The structure was determined by molecular replacement using the PHASER program (Read, 2001); the RT1.A^a-MTF-E structure without the peptide was used as the search MHC model (PDB: 1ED3; Speir et al., 2001). Manual model building was conducted using the Coot software (Emsley et al., 2010) followed by maximum-likelihood refinement with the Buster program (Smart et al., 2012). The final model has been validated using the Protein Data Base validation website and final refinement statistics are summarized in Table S2. All molecular graphics representations were created using PyMol (DeLano, 2002).

Thermal stability assay

Stability of the three peptide-RT1.A^a complexes was assessed using a thermal shift assay. The fluorescent dye Sypro orange was used to monitor the protein unfolding, using a Real Time Detection system (Corbett RotorGene 3000) originally designed for PCR. Each pMHC complex was tested twice at two different concentrations (5 and 10 μM) in duplicate in 10 mM Tris-HCl pH8, 150 mM NaCl. Each pMHC was heated from 25 to 95°C, and the fluorescence intensity measured (excitation at 530 nm, and emission at 555 nm). The Tm, or thermal melting point, represents the temperature for which 50% of the protein is unfolded. The results are reported in Table S1.

QUANTIFICATION AND STATISTICAL ANALYSIS

For the peptide activation test, a non-parametric Wilcoxon signed-rank test, comparing column median to a hypothetical value of 1.0, was done. Statistical significance for the phenotype of activated cells, cytokine expression and proliferation assay was evaluated by a one-tailed Mann Whitney t test. Allo-antibody titration and suppression assay with range of doses were analyzed by Two Way Anova Matched test and Bonferroni post-test. Graft survival was analyzed by Kaplan-Meier log-rank test. Analyses were made with GraphPad Prism 7 software (GraphPad).

DATA AND CODE AVAILABILITY

Data Resources

Crystal structure files for the RT1.Aa/Bu31-10 crystal structure have been deposited in the PDB under accession number 6NF7.